ELSEVIER

Fire Safety Journal **28** (1997) 323–350

0379-7112/97/$17·00

PII:0379-7112(97)00005-2

Fire Detection, Location and Heat Release Rate Through Inverse Problem Solution. Part I: Theory

R. F. Richards, B. N. Munk & O. A. Plumb

School of Mechanical and Materials Engineering, Washington State University, Pullman, WA 99164-2920, USA

(Received 22 February 1996; revised version received 20 November 1996; accepted 16 December 1996)

ABSTRACT

A proposed method of detecting, locating and sizing accidental fires, based on the solution of an inverse heat transfer problem, is described. The inverse heat transfer problem to be solved is that of the convective heating of a compartment ceiling by the hot plume of combustion gases rising from an accidental fire. The inverse problem solution algorithm employs transient temperature data gathered at the ceiling of the compartment to determine the location and heat release rate of the fire. An evaluation of the proposed fire detection system, demonstrating the limits on the accuracy of the inverse problem solution algorithm, is presented. The evaluation involves operating the inverse problem solution algorithm on transient temperature data from computer simulated compartment fires. The simulated fire data are generated assuming fires with quadratic growth rates, burning in a 20 m wide by 20 m deep by 3 m high enclosure with a smooth, adiabatic ceiling. The accuracy of the inverse problem solution algorithm in determining the location of a fire is shown to be insensitive to the errors in the fire model used in the forward problem solution, but sensitive to errors in the measured temperature data. The accuracy of the heat release rate of the fire is sensitive to both errors in the fire model and errors in the temperature data. The validity of the use of computer simulated data in the evaluation is verified with a second evaluation using fire data interpolated from published measurements taken in large-scale compartment fire burns. © 1997 *Elsevier Science Ltd.*

NOTATION

a	Systematic error parameter: constant bias (s)
b	Systematic error parameter: constant fraction
c_1, c_2, c_3, c_4	Correlation constants: eqn (8)

d	Distance between sensors (m)
$G(\sigma)$	Gaussian distribution of random measurement error with standard deviation σ
h	Height of ceiling (m)
l	Length of compartment (m)
n	Number of sensors
Q	Fire heat release rate (W)
Q_{act}	Fire heat release rate reported for large-scale burns in Ref. 8 (W)
Q_{sim}	Simulated fire heat release rate (W)
Q_{pred}	Fire heat release rate predicted by inverse problem solution algorithm (W)
r	Radial distance from fire (m)
S	Sum of squares: eqn (4)
T	Temperature (K)
T_{amb}	Ambient temperature (K)
T_a	Sensor activation temperature (K)
t_i	Predicted activation time of ith sensor (s)
$t_{a,i}$	Predicted elapsed time between activation of ith and first sensors (s)
$\hat{t}_i$	Measured activation time of ith sensor (s)
$\hat{t}_{a,i}$	Measured elapsed time between activation of ith and first sensors (s)
$t_{LAV,i}$	LAVENT simulated elapsed time between activation of ith and first sensors (s)
w	Width of compartment (m)
(x,y)	Fire location (m)
(x_{sim},y_{sim})	Simulated fire location (m)
(x_{pred},y_{pred})	Fire location predicted by inverse problem solution algorithm (m)

Greek letters

α	Fire growth rate ($W s^{-2}$)
α_{sim}	Simulated fire growth rate ($W s^{-2}$)
α_{pred}	Fire growth rate predicted by inverse problem solution algorithm ($W s^{-2}$)
ε_{loc}	Location error (m)
ε_Q	Heat release rate error ratio
σ	Standard deviation of normally distributed random measurement error

1 INTRODUCTION

Industrial facilities such as warehouses and factory floors may combine significant fire risks with minimal human monitoring for extended periods. When accidental fires do occur in industrial settings the time the fire burns undetected plays a crucial role in the destructiveness of the fire. As a result there is a critical need for an economical means to automatically monitor work spaces and quickly determine the presence of a fire and assess the threat to life and property.

Fire protection systems now in service, such as fusible link sprinklers, can automatically detect and act to suppress accidental fires without human intervention. However, these systems have only a rudimentary ability to determine the location and size of the fire. Such systems lack the intelligence to direct suppression measures (automatic or human), so as to maximize fire-fighting effectiveness and minimize collateral damage from water or chemical suppressants. Fire protection systems now being developed are remedying this shortcoming by taking advantage of recent advances in sensor and microprocessor technology. For example, researchers have worked to exploit the power of microprocessors by applying artificial neural networks,[1-3] fuzzy logic,[2,4] statistical methods[5,6] and expert systems[7] to the fire detection problem. These new systems attempt to incorporate intelligence into fire detection systems to enhance their ability to detect a fire quickly, determine its threat and locate the fire, so as to most effectively direct suppression.

Inverse problem solution methods, represent another suite of powerful techniques that can be applied to the problem of fire detection. These methods offer a new approach to introduce an element of intelligence into fire detection systems. The theory of inverse heat transfer problems, is quite well-developed. For example, the recovery of the location and/or heat release rates of heat sources in thermally conducting solids,[8] in radiating gases,[9] and in convective flow situations[10] given a limited number of discrete temperature or heat flux measurements has been demonstrated by various workers.

The heat transfer problem of interest in the problem of fire detection is the convective heating of a compartment ceiling by the buoyant plume and resulting ceiling jet of hot combustion gases originating from an accidental fire. The solution of the inverse heat transfer problem involves comparing transient temperature information gathered by sensors situated at discrete locations on the ceiling to predictions of those temperatures by a numerical fire model. Minimizing the residuals between measured and

predicted temperatures gives the most probable location and heat release rate of the fire which generated the plume and ceiling jet.

In the proposed system transient temperature data are assumed to be collected by n discrete temperature sensors distributed in a square grid across the ceiling of the compartment. The data required by the proposed system are the times at which each sensor reaches a predetermined target temperature. Many potential sensor technologies could be candidates for an actual prototype system. For example, conventional sensors such as thermocouples, or fusible links would serve well as sources of data. Newer technologies to monitor temperature such as fiber optic sensors[11,12] are rapidly appearing. Part II of the present work[13] presents the design and operation of a fire detection system that uses a black and white video camera to gather transient temperature data from color-changing, temperature-sensitive sensors.

In the present work, Part I, the method of solution of the inverse fire detection problem, the inverse problem solution algorithm, is developed. The implementation of the inverse problem solution algorithm in a fire detection system is then described. The limits on the performance of a fire detection system based on the inverse problem solution are evaluated by simulating the operation of the system using computer synthesized fire data. The accuracy of the inverse problem solution based detection system in determining the locations and the heat release rates of the simulated fires is quantified on a statistical basis. Finally, the use of computer simulated fire data in the evaluation of the inverse problem solution algorithm, is validated by comparing the results of the evaluation with a second evaluation based on fire data interpolated from published measurements taken in large-scale experimental compartment fire burns. Part II of this work[13] completes the study, by describing how the inverse problem solution algorithm can be implemented in a working prototype. In the prototype system, the transient temperature information gathered by a video camera monitoring color-changing, temperature-sensitive sensors is used as data in the inverse problem solution algorithm described in the present paper. In addition, Part II reports the results of an evaluation of the accuracy of the prototype in determining the location and heat release rate of small flame sources in reduced-scale fire experiments.

2 SYSTEM DESCRIPTION

The inverse fire detection problem is illustrated in Fig. 1. If a fire is accidentally ignited in a compartment, a buoyant plume of hot combustion gases will be generated. The buoyant plume will rise to the ceiling of the

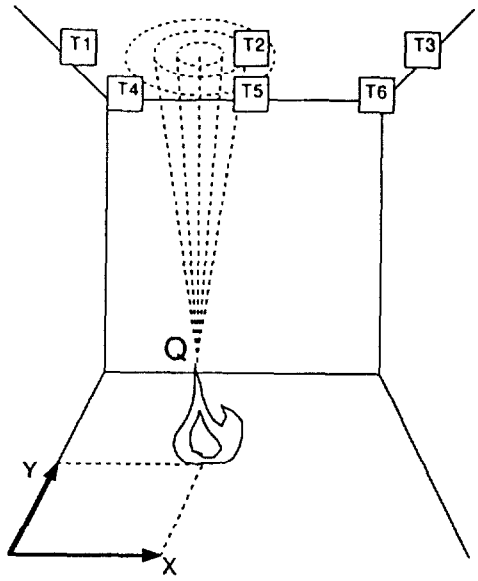

Fig. 1. The inverse fire detection problem.

compartment and upon reaching the ceiling turn and flow radially outward as a ceiling jet. As the ceiling jet spreads radially, the ceiling will be convectively heated. Temperature sensors, T1 through T6, placed at discrete locations on or near the ceiling will also be heated by the ceiling jet. If the temperature sensors are such that they are activated at a temperature between the ceiling jet temperature and ambient temperature, then those sensors will be activated one by one as the ceiling jet spreads radially outward. The inverse problem to be solved is to determine the location, (x,y), and heat release rate, Q, of the fire, given the times at which individual temperature sensors reach their activation temperature.

2.1 Inverse problem solution algorithm

The problem of locating a fire and determining its growth rate can be formally posed as an inverse problem in which the times of activation, t_i, of n ceiling mounted sensors (where $i = 1, n$) are used as data to find two unknown parameters determining the fire location: x, y and one unknown parameter determining the fire growth rate: α. The location of the fire is described by the Cartesian coordinates, (x,y), where the fire is assumed to lie in the plane of the compartment floor. The fire growth rate is

determined by the parameter α, which follows from the functional form of the fire heat release rate assumed in the present work:

$$Q = \alpha t^2 \tag{1}$$

The quadratic form is chosen following Heskestad's recommendation for the initial stages of fire growth.[14] Here Q is the fire's convective heat release rate in W, and t is the elapsed time from the ignition of the fire in seconds. The parameter to be found, α, is seen to have units of $W\,s^{-2}$. The problem is thus one of parameter estimation, with three parameters to be found. It is important to note that the determination of three parameters by inverse problem solution requires no less than four data.

Solution of the inverse problem involves two steps: first prediction of the transient temperature field in the compartment using a numerical fire model and second minimization of the residuals between measured and predicted temperatures to determine the most probable location and heat release rate for the fire. The first step, prediction of the temperature field given the heat source, is commonly referred to as the solution of the forward problem. The second step, comparison of transient temperature data gathered by sensors to predictions of those temperatures by the numerical fire model to obtain location and heat release rate information about the fire, completes the solution of the inverse problem.

In the present study the solution of the forward problem is found using the compartment fire model LAVENT.[15] LAVENT is a two-zone compartment fire model which employs semi-empirical models of the buoyant plume and ceiling jet in order to compute convective heat fluxes from a fire to the ceiling of a compartment. Several assumptions made in the development of LAVENT pose significant restrictions on the problem considered here.

First, LAVENT assumes that the compartment air is quiescent. This assumption implies that room air velocities due to forced air ventilation or induced ventilation from open doors and windows are much smaller than the gas velocities in the buoyant plume rising from the fire. Second, LAVENT assumes that interactions between the plume and side wall are negligible. This assumption limits LAVENT to simulations of fires that are a distance of at least $h/2$ from the compartment side walls. These first two assumptions ensure that both the buoyant plume and ceiling jet remain axially symmetric about a vertical line drawn through the fire. In addition, LAVENT is useful only for simulations in the early stages of a compartment fire, before the top of the flame begins to reach the compartment ceiling.

LAVENT assumes that the compartments considered have a plan aspect ratio not far from unity. Compartments need not be square, but must

have an aspect ratio in the range $1 \leq l/w \leq 2$. As a result fires in long hallways or corridors can not be simulated. The compartment considered must have a smooth ceiling, without solid beams or other architectural elements which would pose barriers to the flow of the ceiling jet radiating from the fire plume.

Forward problem solutions are found for a set of many fire scenarios. Each fire scenario consists of a fire with a given location and growth rate, (x,y,α), in the relevant compartment geometry. The zone fire model LAVENT, is employed to predict the transient temperature field across the compartment ceiling for each fire scenario (x,y,α) in the set. Using the transient temperature solution for each scenario from LAVENT, the times at which each sensor will be activated can be determined, given both the locations of the temperature-sensitive sensors and their activation temperature. The predicted activation time for each sensor is then defined to be the elapsed time between the activation times of the particular sensor and the first sensor activated:

$$t_{a,i} = t_i - t_1 \tag{2}$$

Note that n sensor activation times, t_i, yield $(n-1)$ predicted activation times, $t_{a,i}$, since the predicted activation time of the first sensor is always zero.

The collection of predicted activation times covering all possible fire scenarios constitutes the database of forward problem solutions used for the inverse problem solution. In the present study a complete set of fire scenarios consists of eight discrete fire growth rates in the range $0{\cdot}001 < \alpha < 0{\cdot}06\,\mathrm{kW\,s^{-2}}$, and 400 fire locations situated on a square grid at increments of $0{\cdot}05d$ (where d is the distance between sensors) in x and y. Due to symmetry only 66 of the 400 fire locations are unique. Therefore, a complete set of forward problem solutions involves a database of only 528 fire scenarios. Forward problem solutions can be pre-calculated and stored in computer memory. For each different compartment geometry, size, or set of detector locations a separate set of forward problem solutions must be generated and stored.

The solutions are stored in the form of the locations and activation times of the first five sensors to be set off by the fire: $(x_i,y_i,t_{a,i})$ where $i = 1$–5. Activation times, t_i, for five sensors are required, since five activation times yield four predicted activation times, $t_{a,i}$. Four predicted activation times are the minimum number of data required to solve the inverse problem for the three unknown parameters, (x,y,α). In general, if more data were used in the inverse problem solution, better estimates of the unknown parameters would result.

Given a complete set of forward solutions, the second step of the

inverse problem solution algorithm can be implemented: the comparison of measured and predicted transient temperature data. The data required for the inverse problem solution are the times at which individual sensors are activated as a result of the plume of hot gases rising from the fire. Measured activation times for the first five sensors activated ($i = 1$–5) in a given fire scenario are required, where the measured activation time for each sensor is taken as the elapsed time from the time the first sensor is activated:

$$\hat{t}_{a,i} = \hat{t}_i - \hat{t}_1 \tag{3}$$

Once again, note that n sensor activation times, $\hat{t}_i$, yield $(n-1)$ measured activation times, $\hat{t}_{a,i}$.

The inversion algorithm proceeds by subtracting measured activation times from predicted activation times and then summing the squares of the differences:

$$S = \sum_{i=1}^{n} (t_{a,i} - \hat{t}_{a,i})^2 \tag{4}$$

The solution to the inverse problem is taken to be the values of the parameters x, y and α for the fire scenario which minimizes the sum of squares, S, over the complete set of fire scenarios. The minimum of S is found through the technique of exhaustive search. The sum of squares, S, is calculated for each of the 528 fire scenarios in a complete set and the minimum value found by comparing the values of S determined for each scenario. In those cases where two or more fire scenarios produce equal minima of S, the average of the respective values of x, y and α are taken as the solution.

The solution of an inverse problem proceeds by matching measured data with values predicted by a forward problem model. As a result, the accuracy of the inverse problem solution is closely tied to the accuracy of the forward problem model. In the present study, it is the accuracy of the compartment fire zone model, LAVENT, in predicting the heat and mass transfer from a fire to the compartment ceiling via the buoyant fire plume and the resulting ceiling jet, that is pivotal in the solution of the inverse fire detection problem.

3 INVERSE PROBLEM SOLUTION ALGORITHM EVALUATION

Two tests were undertaken to evaluate the inverse problem solution algorithm. First, the accuracy of the algorithm was evaluated using

computer simulated fire data. Second, the use of the computer simulated data to test the algorithm was validated using fire data interpolated from measurements taken in full scale experimental burns.

The accuracy of the inverse problem solution algorithm in locating and sizing accidental fires largely depends on the algorithm's sensitivity to two kinds of error: random errors in the transient temperature measurements and the systematic errors in the forward problem solution. Random errors in sensor activation times must be expected regardless of the type of sensor used to gathered the data required by the inversion algorithm. Likewise, any fire model used to produce the forward problem solution will have associated with it some limitations, assumptions, or simplifications which will result in systematic errors in that solution.

To evaluate the performance of the inverse problem solution algorithm, the algorithm was exercised on test cases consisting of computer simulated fire data. Quantification of the effect of the errors described above, was accomplished by corrupting the original simulated fire data by adding to the data random and systematic errors of known magnitude. The fire location and heat release rate predicted by the inverse problem solution algorithm using the corrupted fire data (data with errors) was then compared to the fire location and heat release rate which was assumed to produce the original uncorrupted fire data.

3.1 Fire detection system simulation

The evaluation began by simulating a compartment fire with given location and growth rate (x,y,α) using the zone fire model LAVENT. Sensor activation times were determined given the sensor location and the transient temperature field at the compartment ceiling calculated by LAVENT for a fire with the assumed location and growth rate.

All simulations were run assuming a compartment similar to the warehouse used for the large-scale test burns at the Factory Mutual Research Center reported by Heskestad and Delichatsios.[16] The compartment was taken to be 3 m high, 20 m wide and 20 m deep, with a smooth, insulated ceiling. The compartment was assumed to be completely enclosed, without sources of ventilation, so that the air in the compartment was quiescent.

The compartment geometry met the restriction on LAVENT that compartments must have aspect ratios in the range $1 \leq l/w \leq 2$. The smooth ceiling met the restriction that there be no architectural elements which would pose a barrier to the flow of the ceiling jet. The assumption

of quiescent air in the compartment was required, because LAVENT i based on the assumption that room air velocities are much smaller tha the gas velocities of the buoyant plume rising from the fire. Plum velocities for the fire scenarios simulated in the present work were on th order of $1\ m\ s^{-1}$.

LAVENT simulations were continued only until the fires were detected located and sized. During the study, it was not necessary to run an simulation longer than 3 min from the time of ignition and no fir simulated grew larger than 100 kW, before being detected and located. A a consequence of the fact that the present work focused on early fir detection, assumptions limiting LAVENT to simulations of the earl stages of fire growth were not significantly restrictive.

The ambient temperature in the compartment was taken to be constan at $T_{amb} = 300\ K$. The temperature sensors for the detection system were assumed to be distributed on a square grid, spaced three meters apart. The activation temperature for all sensors was selected to be $T_a = 311\ K$. The sensors were assumed to hang in the hottest part of the ceiling jet, between 0 and 10 cm from the ceiling. The sensors were taken to have negligibly small thermal mass, so that their time response would be essentially instantaneous. However, the time of activation was always rounded to the nearest second, to account for the finite speed of data acquisition systems.

3.2 Error simulation

To enable the quantification of the effects of uncertainty that would inevitably arise in a real fire detection system, errors were added to the sensor activation times determined from the LAVENT simulated fire data. In this way corrupted data were produced which more closely resembled sensor activation times that would be measured during a real fire, than the original LAVENT simulated data.

Two types of error were added to the LAVENT simulated data. To account for limitations or inaccuracy inherent in the fire model used to produce the forward solution, a systematic error was added to the simulated sensor activation times. The systematic model error was assumed to be composed of a constant bias and a component which grew linearly in elapsed time. To account for uncertainty in the sensor activation time measurements, a random error was also added to the LAVENT simulated activation times. The random measurement errors, were assumed to follow a Gaussian distribution with a mean value of zero. Adding the systematic and random errors to the original LAVENT

simulation activation time for the ith sensor, $t_{LAV,i}$, the corrupted activation time of the ith sensor, $t_{a,i}$ could be calculated:

$$\hat{t}_{a,i} = \hat{t}_{LAV,i} + (a + b\hat{t}_{LAV,i}) + G(\sigma) \tag{5}$$

where a and b are constants characterizing systematic error and $G(\sigma)$ is a random number chosen from a normal distribution with standard deviation σ. Note that the parameter a has units of seconds and represents a constant time bias. The parameter b, which has a dimensionless value between zero and unity, represents an error which is always a constant fraction of the elapsed time.

3.3 Inverse algorithm test

A test of the inverse problem solution algorithm was run by randomly selecting a fire location, (x_{sim},y_{sim}), in the range $0 < x_{sim} < d$, $0 < y_{sim} < d$ and a fire growth rate, α_{sim}, in the range $0{\cdot}001 < \alpha_{sim} < 0{\cdot}06\,\text{kW s}^{-2}$. LAVENT was run to simulate the transient temperature history at the compartment ceiling for the given fire location and growth rate. The LAVENT generated transient temperatures were then used to determine sensor activation times, $t_{LAV,i}$, for the five sensors nearest to the fire ($i = 1$–5). Random and systematic errors were added to the LAVENT simulated sensor activation times, to produce the corrupted sensor activation times, $t_{a,i}$, using eqn (5). The inverse problem solution algorithm was then employed, using the corrupted sensor activation times, $t_{a,i}$, as data, to predict a fire location and heat release rate, $(x_{pred},y_{pred},\alpha_{pred})$.

The accuracy of the inverse problem solution algorithm was scored by calculating the errors in the algorithm's predictions of the fire location and heat release rate. The location error, ε_{loc}, was defined to be the distance between the fire location (x_{pred},y_{pred}) predicted by the inverse problem solution algorithm and the location (x_{sim}, y_{sim}) originally selected to produce the simulated sensor times to activation:

$$\varepsilon_{loc} = \sqrt{(x_{pred} - x_{sim})^2 + (y_{pred} - y_{sim})^2} \tag{6}$$

where ε_{loc} was measured in centimeters. For a perfect fire detection system with no error, the location error was zero, $\varepsilon_{loc} = 0$ cm.

The heat release rate error ratio, ε_Q, was defined to be the ratio of the heat release rate of the fire, predicted by the inverse problem solution algorithm, $Q_{pred}(t_{a,5})$, over the heat release rate of the fire originally

simulated, $Q_{sim}(t_{a,5})$, where both heat release rates were calculated at the time of the activation of the fifth sensor:

$$\varepsilon_Q = Q_{pred}(t_{a,5})/Q_{sim}(t_{a,5}) \tag{7}$$

As defined, the heat release rate error ratio was dimensionless. Note that for cases where the predicted heat release rate, $Q_{pred}(t_{a,5})$, and the simulated heat release rate, $Q_{sim}(t_{a,5})$, diverged, the value of heat release rate error ratio, ε_Q, shifted away from unity. Heat release rate error ratios less than unity meant that the inverse problem solution algorithm had underpredicted the fire size, while ratios greater than unity meant that the algorithm had overpredicted fire size.

The inverse problem solution algorithm was run using data from 1000 different simulated fires to provide an ensemble of results at each set of test conditions. The location, (x,y) of each of the simulated fires was randomly chosen, while the growth rate, α, of the fires was kept constant over all of the 1000 simulated runs. A set of test conditions consisted of the specified magnitudes of random error and systematic error added to the simulated fire data, along with the fire growth rate. Since random error is determined by the standard deviation, σ, of the Gaussian distribution $G(\sigma)$, while systematic error is controlled by the constants b and c in eqn (5) a test condition is specified by the set of parameters: (α, σ, b, c). Location and heat release rate error statistics for each test condition were determined from the ensemble of errors resulting from the 1000 simulated test fire runs.

3.4 Validation of the inverse algorithm evaluation

The usefulness of the results of the evaluation of the inverse problem solution algorithm just described, depends upon the degree to which the computer simulated fire data used in the evaluation resembles real data produced by real fires. To validate the use of simulated fire data in the evaluation of the algorithm and to verify that such an evaluation yields realistic results, a parallel evaluation based on experimental measurements was undertaken. Measurements made during large scale test burns of wood crib fires at the Factory Mutual Research Center by Heskestad and Delichatsios[16] provided a set of realistic fire data. In that paper, measurements of ceiling jet temperatures were given versus time and radius from the fires, for eight different fires. Unfortunately, the ceiling jet temperatures reported in Heskestad and Delichatsios[16] were given at only six radial locations. As a result, a means to 'interpolate' transient temperature data, at radial distances between those distances for which Heskestad and Delichatsios[16] reported measurements, was employed.

The interpolation of transient temperature data from the

measurements was accomplished by fitting the measurements to a general form of the correlation given as eqn (1) in Heskestad and Delichatsios.[16]

$$t(r) = c_1(T(r) - T_{amb})^{3/4} + c_2(T(r) - T_{amb})^{3/4}(r/h) + c_3(r/h) + c_4 \qquad (8)$$

where $T(r)$ is the ceiling jet temperature at radius r, $t(r)$ is time elapsed from the start of the fire, h is the ceiling height, and c_1, c_2, c_3 and c_4 are constants. In the present work, elapsed time is chosen as the dependent variable and temperature as the independent variable, because the inversion algorithm uses as data the times at which sensors at various radii from the fire plume reach their activation temperature. Once the correlation, eqn (8), was fitted to the measurements from Heskestad and Delichatsios[16] using least squares, residuals for the data with respect to the correlation were calculated. The residuals were tabulated by counting the number of residuals that fell into bins between the lowest and highest values of the residuals ($-12 < r < 10$ s), where each bin was 1 s wide. Figure 2 shows the resulting probability density function for the residuals. For comparison, a Gaussian distribution with a mean value of 0 s and standard deviation of 4·7 s is shown on the same figure.

Using eqn (8) with the appropriate constants c_1, c_2, c_3 and c_4, and the residual pdf given in Fig. 2, it was possible to generate new time versus temperature data. The new data was generated by using the correlation to calculate a time, $t(r)$, at which a given temperature, $T(r)$, would be reached at any radial position, r. Values randomly chosen from the residual pdf (Fig. 2) were then added to the time, $t(r)$, resulting from the

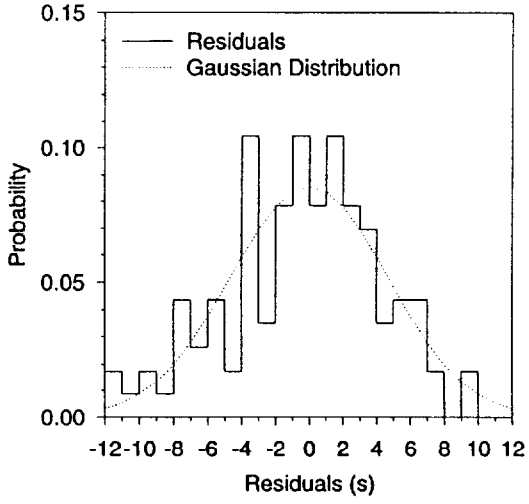

Fig. 2. Residual probability distribution function determined from the difference between large-scale fire test data taken from Ref. 16 and eqn (8). A Gaussian distribution with mean value 0 s, and standard deviation $\sigma = 4{\cdot}7$ s is shown for comparison.

correlation. Time versus temperature data generated in this way would be indistinguishable from the original measurements reported in Heskestad and Delichatsios.[16]

4 RESULTS

4.1 Fire location accuracy

The accuracy of the inverse problem solution algorithm in locating fires can be assessed by referring to Figs 3 and 4, where statistics on fire location error from 1000 simulated test fires are shown. Consider first Fig. 3(a, b), where the effect of random errors and systematic errors on the inversion algorithm's accuracy in predicting fire location is illustrated. In the figures, probability density functions for location error are shown for both slow-growing ($\alpha = 2{\cdot}98\ \mathrm{W\,s^{-2}}$) and fast-growing ($\alpha = 42{\cdot}6\ \mathrm{W\,s^{-2}}$) fires given. Location errors are reported as the distance between predicted and actual fire locations and given in centimeters.

The effect of random error is shown in Fig. 3(a). In that figure, where no systematic error has been added (LAVENT is assumed to be a 'perfect' fire model), probability density functions of location error for simulations of fires with no random error ($\sigma = 0\,\mathrm{s}$) and with moderate random error ($\sigma = 5\,\mathrm{s}$), are given. With no random error ($\sigma = 0\,\mathrm{s}$), although most fires are located exactly, a few fires are found with location errors of as much as 30 cm. This small location error is due to the fact that sensor activation times are rounded off to the nearest second, to account for the finite speed of the data acquisition equipment. As random measurement error is increased from $\sigma = 0\,\mathrm{s}$ to $\sigma = 5\,\mathrm{s}$, however, errors in the fire location predicted by the inverse problem solution algorithm begin to increase more significantly. The effect is seen to be greater for fast-growing fires than for slow-growing fires.

Figure 3(b) shows the effect of systematic or model error on the accuracy of the inversion algorithm to predict the fire location. Pdfs of location error are given for cases of fire data for slow-growing fires with systematic error corresponding to (1) $a = 0\,\mathrm{s}$, $b = 0$, (2) $a = 40\,\mathrm{s}$, $b = 0$, and for fast-growing fires with systematic error corresponding to (1) $a = 0\,\mathrm{s}$, $b = 0$, (2) $a = 0\,\mathrm{s}$, $b = 0{\cdot}6$. In all cases an added random error of $\sigma = 5\,\mathrm{s}$ is included. Location errors are seen to be larger for fast-growing fires than for slow-growing fires as in Fig. 3(a). However, in contrast to the previous case, fire location errors do not increase as systematic model error increases. In fact, for the fast-growing fires, location errors decrease slightly when the parameter b is increased. This conclusion can be seen more clearly in Fig. 4(a,b).

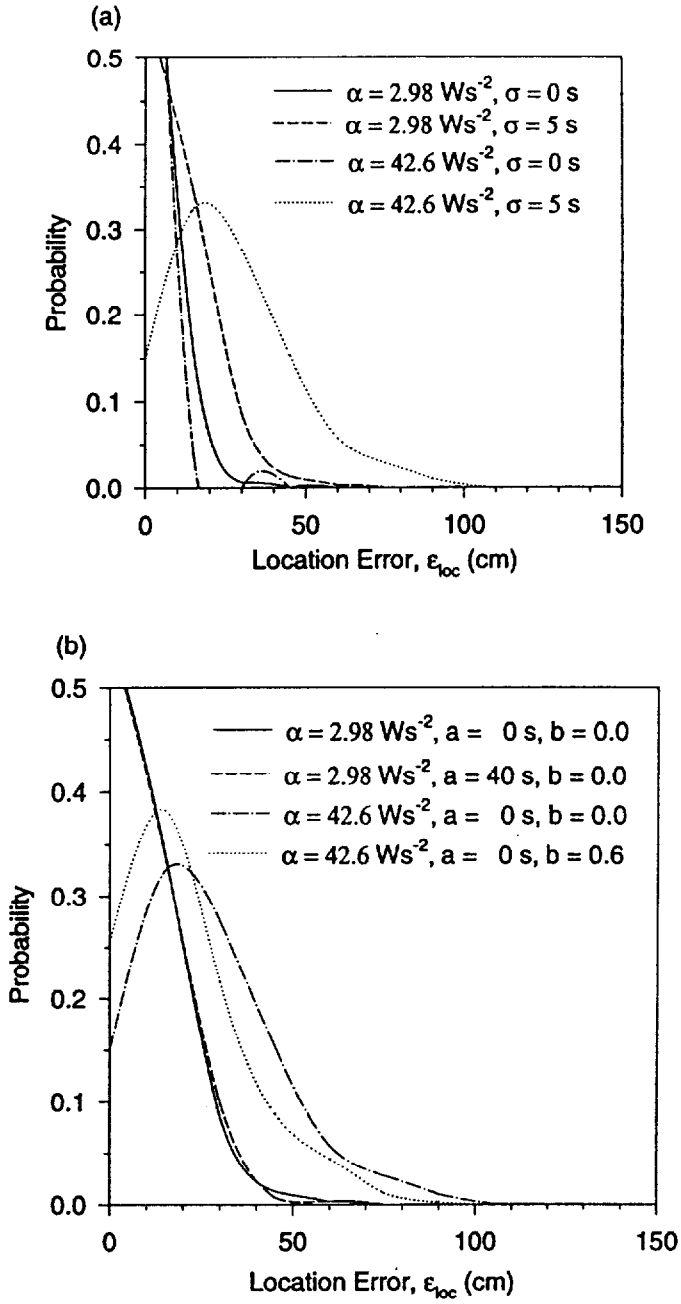

Fig. 3. (a) Location error pdfs for slow and fast-growing fires: $\alpha = 2{\cdot}98\ \mathrm{W\,s^{-2}}$ and $\alpha = 42{\cdot}6\ \mathrm{W\,s^{-2}}$ at two levels of random error: $\sigma = 0$ s and $\sigma = 5$ s, and no systematic error. (b) Location error pdfs for slow and fast-growing fires: $\alpha = 2{\cdot}98\ \mathrm{W\,s^{-2}}$ and $\alpha = 42{\cdot}6\ \mathrm{W\,s^{-2}}$ at three levels of systematic error: $a = 0$ s, $b = 0{\cdot}0$; $a = 40$ s, $b = 0{\cdot}0$; $a = 0$ s, $b = 0{\cdot}6$ and random error $\sigma = 5$ s.

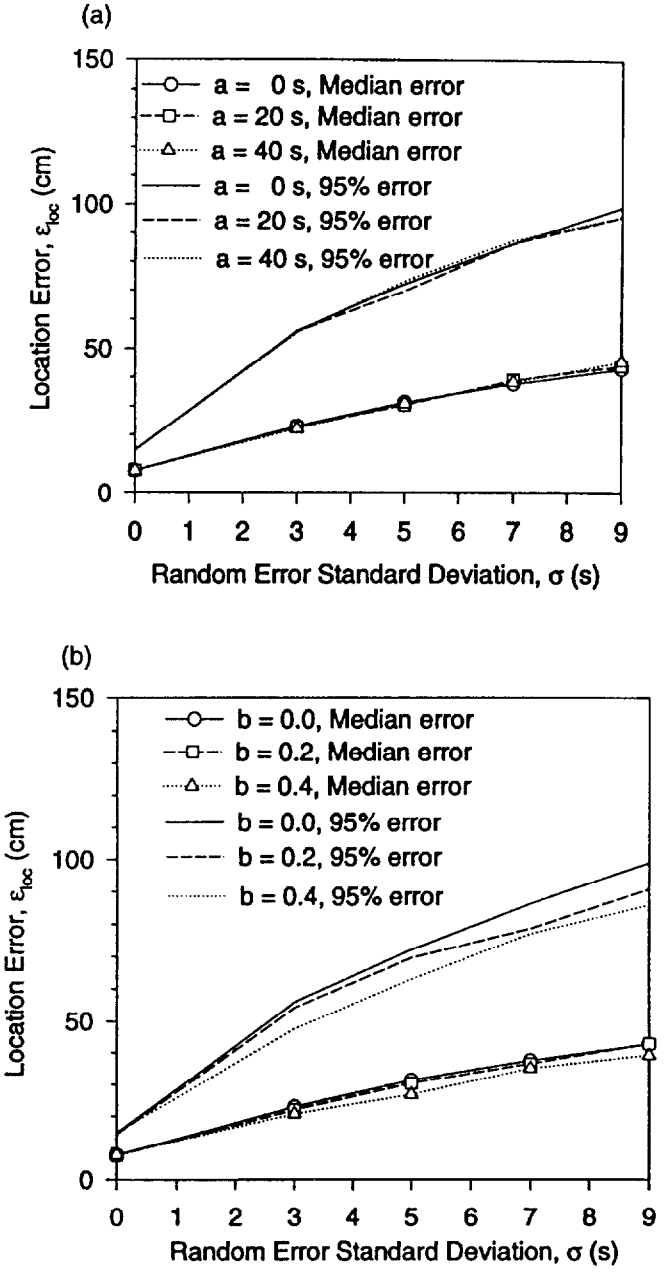

Fig. 4. (a) Median location error with 95% confidence interval versus random error, for fast-growing fires: $\alpha = 42.6\ \mathrm{W\,s^{-2}}$ for three levels of systematic error: $a = 0$ s, $b = 0{\cdot}0$; $a = 20$ s, $b = 0{\cdot}0$; and $a = 40$ s, $b = 0{\cdot}0$. (b) Median location error with 95% confidence interval versus random error, for fast-growing fires: $\alpha = 42{\cdot}6\ \mathrm{W\,s^{-2}}$ for three levels of systematic error: $a = 0$ s, $b = 0{\cdot}0$; $a = 0$ s, $b = 0{\cdot}2$; and $a = 0$ s, $b = 0{\cdot}40$.

In Fig. 4(a,b) both the median error and the 95% confidence intervals about the median error in fire locations predicted by the inverse problem solution algorithm are plotted versus random error standard deviation, σ. Only results for fast-growing fires ($\alpha = 42{\cdot}6\ \mathrm{W\,s^{-2}}$) are shown. The median location error represents an error greater than the location errors found for 50%, or 500 out of 1000 test fires. Likewise, the 95% confidence interval represents a location error greater than the location errors for 95%, or 950 out of 1000 fires in a test run. In Fig. 4(a) location error is plotted for three cases of systematic error: $a = 0$, 20, 40 s with $b = 0{\cdot}0$ while in Fig. 4(b) location error is plotted for three other cases of systematic error: $a = 0$ s with $b = 0$, 0·2, 0·4. Both figures clearly demonstrate that varying systematic error by changing parameters a and b has little effect on either the median or the 95% confidence intervals for location errors. On the other hand, increasing the random error standard deviation, σ, causes monotonic increases in both the inversion algorithm's median location error and 95% confidence interval on location error.

The insensitivity of inverse algorithm location error to systematic model error and the sensitivity of the location error to random measurement error are both consequences of the fact that the algorithm predicts fire location primarily on the basis of the order in which sensors are activated. For example, the inverse algorithm will always predict the fire to be closest to the sensor which is activated first, the fire to be next closest the sensor activated second and so on. The algorithm predicts fire location secondarily on the relative elapsed times between activation of sensors. That is, the longer it takes for a sensor to activated, the farther that sensor must be from the fire. All radially symmetric compartment fire models will predict the same sequence of sensor activations for a given fire location. All radially symmetric compartment fire models will predict that the greater the distance from the fire to any given sensor the greater the elapsed time until the sensor is activated. For these reasons, the particular fire model used in the inverse problem solution algorithm will have little effect on the fire location predicted. In the same way, systematic errors in the fire model will have little effect on fire location errors, as seen in Fig. 4(a,b).

The effect of random errors is quite different. Random measurement errors will cause the relative times of activation of sensors to vary from their 'true' values. A random measurement error causing the apparent activation time of a sensor to be sooner than the actual elapsed time will shift the predicted fire location closer to that sensor. A random error causing a sensor activation time to appear later than the actual time will shift the predicted fire location away from that sensor. In the case of large random measurement errors the sequence of two sensor activations may

even be reversed. The increase in fire location error with increased random measurement errors seen in Fig. 4(a,b) reflects these mechanisms.

4.2 Fire heat release rate accuracy

The effect of random and systematic errors on the accuracy of the inversion algorithm in predicting fire heat release rates for fast- and slow-growing fires is shown in Fig. 5(a,b). In the figures, heat release rate error ratio probability density functions are given, where heat release rate error ratio is reported as the heat release rate predicted by the inversion algorithm, divided by the actual fire's heat release rate, at the time of the fifth sensor activation. The effect of random error is shown in Fig. 5(a) where heat release rate error ratio pdfs are given for fire data with $\sigma = 0$ and 5 s, and with no systematic error (perfect fire model). Increasing random measurement error is seen to have little effect on the peak of the heat release rate error ratio pdf, while causing the width of the pdf to grow. The increase in pdf width is larger for fast-growing fires than for slow-growing fires. For example, the pdf for the fast-growing fires spreads from 0·5 to 1·9, with a peak at 1·0, while the pdf for the slow-growing fires spreads only from 0·7 to 1·4, with a peak at 0·95.

The effect of systematic error is shown in Fig. 5(b). In the figure, heat release rate error ratio pdfs are given for cases of systematic error corresponding to slow-growing fires with: (1) $a = 0$ s, $b = 0$, (2) $a = 40$ s, $b = 0$, (3) and fast-growing fires with: (1) $a = 0$ s, $b = 0$, (2) $a = 0$ s, $b = 0{\cdot}6$, for fire data with added random error of $\sigma = 5$ s. Increasing systematic error causes the peak of the heat release rate error ratio pdf to shift away from unity to smaller values. The shift in the peak of the pdf is greater for fast-growing fires, with the peak of the pdf for the fast-growing fires shifting from 1·0 to 0·35 while the peak of the pdf for slow-growing fires shifts only from 0·95 to 0·6. Interestingly, the width of the pdf appears to decrease with increasing systematic error for both fast- and slow-growing fires. For example the pdf for the fast-growing fires covers from 0·5 to 2·0, for the case with no systematic error. Introducing a systematic error characterized by $b = 0{\cdot}6$ shrinks the pdf so that it stretches only from 0·2 to 0·8. Likewise for slow-growing fires with no systematic error, the pdf covers from 0·7 to 1·5. Introducing a systematic error characterized by $a = 40$ s, shrinks the pdf, so that it covers only from 0·45 to 0·9. However, even though the absolute width of the heat release rate error pdf decreases with increased systematic error, the width of the heat release rate error ratio pdf normalized by the mean value of the heat release rate error ratio remains constant. This can be seen in Fig. 6(a,b).

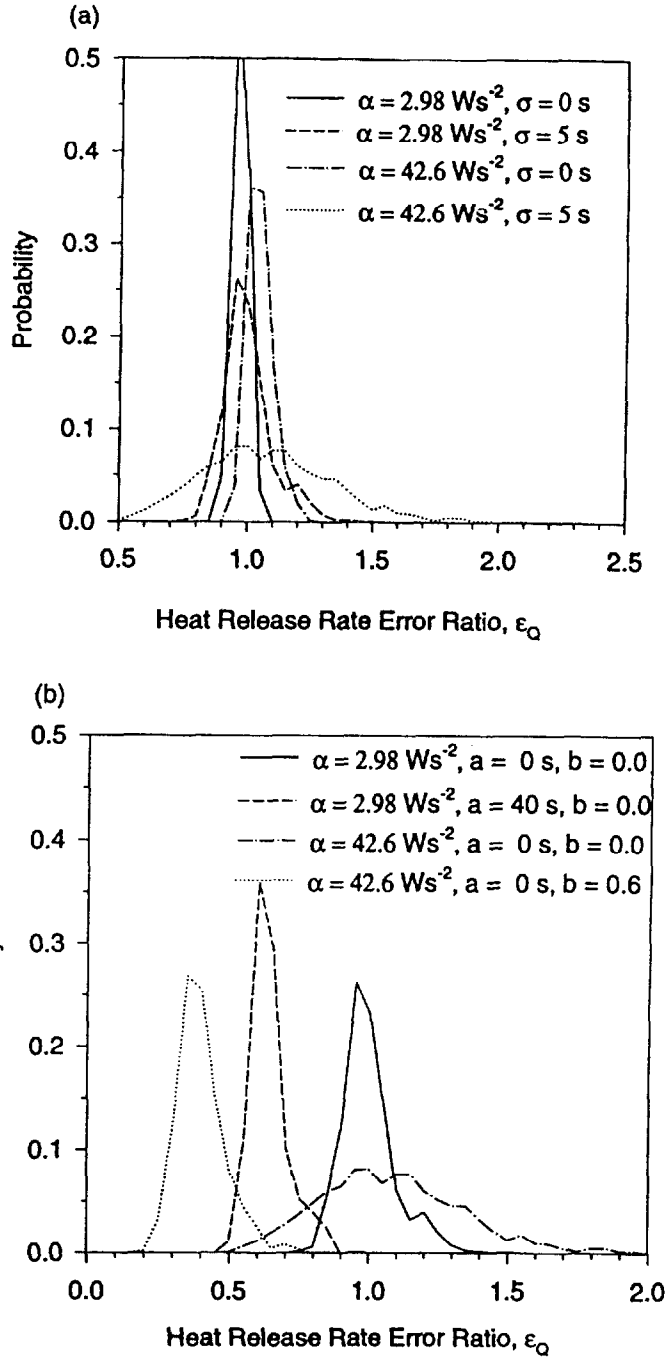

Fig. 5. (a) Heat release rate error pdfs for slow- and fast-growing fires: $\alpha = 2{\cdot}98\ \mathrm{W\,s^{-2}}$ and $\alpha = 42{\cdot}6\ \mathrm{W\,s^{-2}}$ at two levels of random error: $\sigma = 0$ s and $\sigma = 5$ s, and no systematic error. (b) Heat release rate error pdfs for slow- and fast-growing fires: $\alpha = 2{\cdot}98\ \mathrm{W\,s^{-2}}$ and $\alpha = 42{\cdot}6\ \mathrm{W\,s^{-2}}$ at three levels of systematic error: $a = 0$ s, $b = 0{\cdot}0$; $a = 40$ s, $b = 0{\cdot}0$; $a = 0$ s, $b = 0{\cdot}6$ and random error $\sigma = 5$ s.

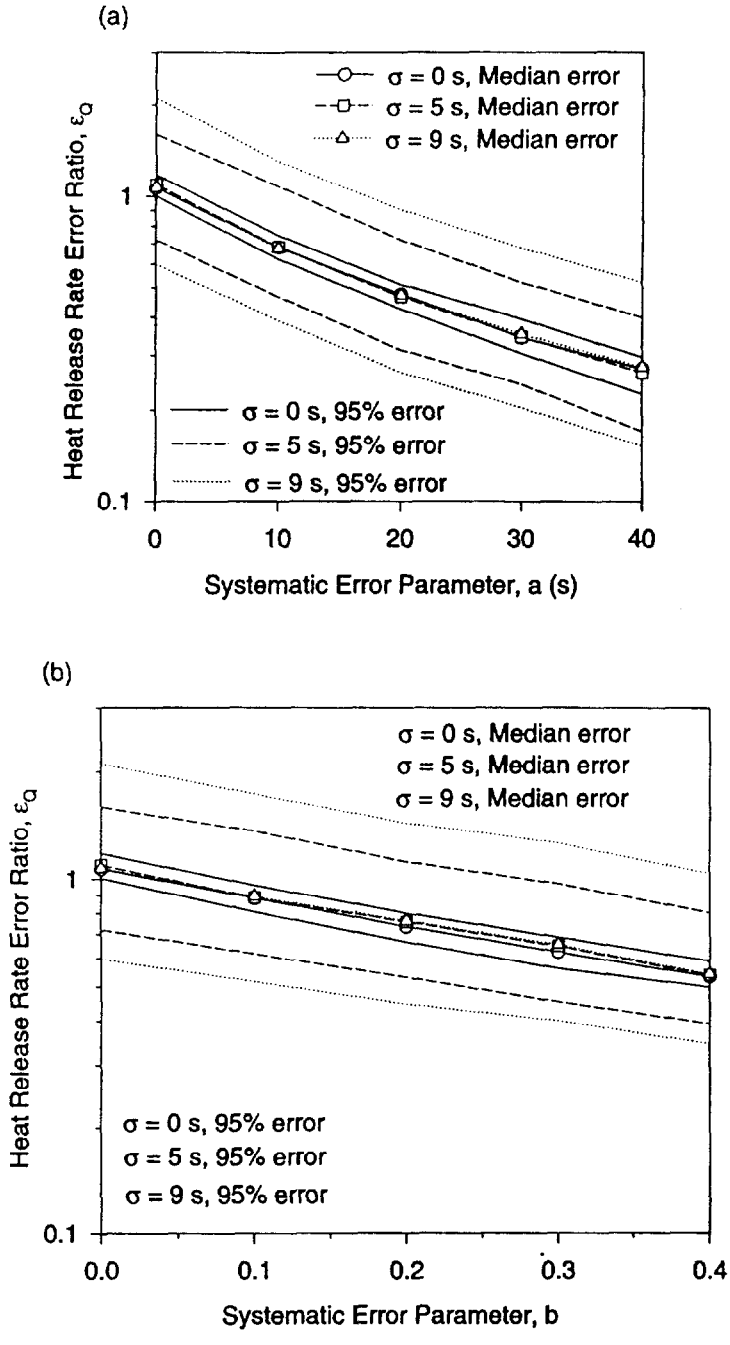

Fig. 6. (a) Median heat release rate error with 95% confidence interval versus systematic error parameter, a, for fast-growing fires: $\alpha = 42{\cdot}6\ \mathrm{W\,s^{-2}}$ for three levels of random error: $\sigma = 0$ s, $\sigma = 5$ s and $\sigma = 9$ s. (b) Median heat release rate error with 95% confidence interval versus systematic error parameter, b, for fast-growing fires: $\alpha = 42{\cdot}6\ \mathrm{W\,s^{-2}}$ for three levels of random error: $\sigma = 0$ s, $\sigma = 5$ s and $\sigma = 9$ s.

Figure 6(a,b) gives semi-logarithmic plots of median error and 95% confidence intervals about the median error for predicted heat release rate error ratio versus systematic error. In Fig. 6(a) heat release rate error ratio is plotted on a log scale against the systematic error parameter, a, ($b = 0$) for three cases of random error: $\sigma = 0$, 5, 9 s. In Fig. 6(b) heat release rate error is plotted on a log scale against the systematic error parameter, b, ($a = 0$) for the same three cases of random error: $\sigma = 0$, 5, 9 s. In both figures results are shown for fast-growing fires ($\alpha = 42{\cdot}6\ \mathrm{W\,s^{-2}}$) only.

Figure 6(a,b) shows a very different behavior for heat release rate errors than Fig. 4(a,b) showed for location errors for the inverse problem solution algorithm. Recall that Fig. 4(a,b) showed that location errors were sensitive to random measurement errors, but insensitive to systematic errors in the fire model. Figure 6(a,b) shows that median errors in heat release rate are sensitive to systematic model error (changes in either a or b) and are insensitive to random measurement error (changes in σ). In contrast, the 95% confidence intervals on heat release rate error, as seen on the semi-log plots, are insensitive to systematic model error (changes in a or b) and are sensitive to random measurement error (changes in σ). In other words, increasing systematic model error (parameters a and b) will cause the peak of the heat release rate error pdf to shift to successively smaller values of ε_Q, where the smaller the value of ε_Q, the more the inverse problem solution algorithm is underpredicting the fire size. At the same time, increasing systematic model error will have no effect on the width of the pdf as seen on the semi-log plot, where a constant width implies a constant ratio between the median error ratio and the 95% error ratio. In contrast, increasing random measurement error will have no effect on the position of the peak of the heat release rate error pdf, while causing the width of the pdf to increase.

The accuracy of fire heat release rates predicted by the inverse problem solution algorithm is tied closely to the accuracy of the forward model (in the present case: LAVENT) used by the algorithm. The accuracy of fire locations predicted by the inverse algorithm does not depend on the accuracy of the forward model. If the forward model overpredicts compartment ceiling temperatures then the inverse problem solution algorithm will consistently underpredict fire heat release rate, but may still accurately predict the fire location. This is precisely the meaning of Fig. 4(a,b) and Fig. 6(a,b). The dependence of fire heat release rate predictions on forward model accuracy, in contrast to the independence of fire location predictions from forward model accuracy, makes the determination of fire size a much more difficult task than the determination of fire location, for a practical fire detection system.

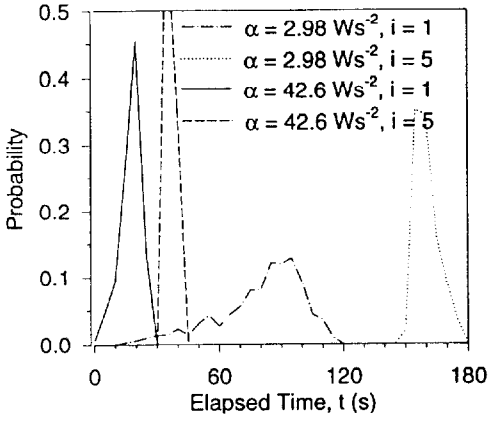

Fig. 7. Sensor time to activation pdfs for first and fifth sensors.

4.3 Speed of fire detection

The speed with which the proposed fire detection system can locate and size a fire is of interest. Figure 7 shows probability density functions for activation times of the first and fifth sensors for a slow-growing fire ($\alpha = 2{\cdot}98\ \mathrm{W\,s^{-2}}$) and a fast-growing fire ($\alpha = 42{\cdot}6\ \mathrm{W\,s^{-2}}$) for 1000 test runs. Upon activation of the first sensor the system has its first evidence of the fire. Upon activation of the fifth sensor the inversion algorithm has sufficient information to locate the fire. The slow-growing fire is seen to be first detected within 2 min and located and sized within 3 min. The fast-growing fire is first detected within 30 s and located and sized within 50 s.

Figure 7 also demonstrates why location and heat release rate errors are greater for fast-growing fires than for slow-growing fires given equal magnitudes of random and systematic error. Consider, for example, a case in which sensor activation times for both fast- and slow-growing fires have associated with them random error with $\sigma = 5$ s. The mean time of activation of the first sensor is 19 s for the fast-growing fire and 37 s for the slow-growing fire. The random error then is 26% of the activation time for the fast-growing fire, but only 14% of the activation time for the slow-growing fire. Likewise, a systematic error consisting of a constant bias of $a = 5$ s would constitute a much larger fraction of the sensor activation times for fast-growing fires than for slow-growing fires. It is the ratio of activation time errors to the activation times themselves and not the absolute magnitude of the errors which controls the accuracy of the inverse problem solution algorithm. This ratio will always be larger for

fast-growing fires than for slow-growing fires given equal random and systematic errors. Figure 3(a,b) and Fig. 5(a,b) reflect this fact.

4.4 Evaluation validation

The validity of the use of simulated fire data in the evaluation of the inverse problem solution algorithm was investigated. Results of the evaluation using simulated data were compared to an evaluation using data interpolated from experimental measurements taken in a large-scale compartment fire test, as reported in Heskestad and Delichatsios.[16]

The method of interpolation of data from actual measurements using the correlation given as eqn (8) in conjunction with the time residual pdf has been described in Section 3.4. It is important to emphasize here that although the interpolated sensor activation time data are not experimental measurements, the data were developed directly from, and closely resemble, the original measurements. To judge how closely the interpolated data resemble the original data from Heskestad and Delichatsios,[16] a comparison between some of the original measurements and the interpolated data is given in Fig. 8. In the figure, data from Heskestad and Delichatsios[16] in the form of time versus temperature measurements for three radial locations on the ceiling above a fast-growing ($\alpha = 42{\cdot}6\ \mathrm{W\,s^{-1}}$)

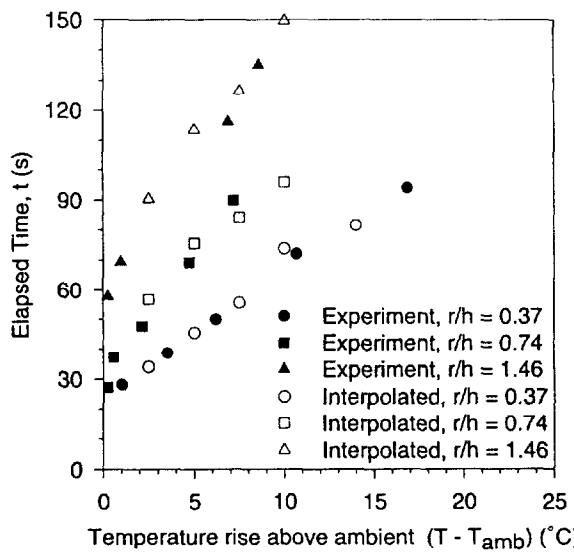

Fig. 8. Comparison of experimental measurements taken from Ref. 16 and interpolated data produced using eqn (8) and the residual probability distribution function.

compartment fire are plotted with filled symbols. On the same figure, data interpolated from the experimental measurements using the method of Section 3.4, are plotted with open symbols. The comparison between the interpolated data and the original measurements from which they were derived is seen to be quite good.

Results of the evaluation of the inverse problem solution algorithm based on interpolated data, similar to the data shown in Fig. 8, are given in Fig. 9(a,b), alongside results from an evaluation using computer simulated data. The figures show pdfs for location errors and heat release rate error ratios for the inverse problem solution algorithm, when locating and sizing 1000 randomly-located, fast-growing fires ($\alpha = 42{\cdot}6\ \mathrm{W\,s^{-1}}$). Solid lines show results from the evaluation using interpolated fire data. Dashed lines show results from the evaluation using computer simulated fire data. The computer simulated data, produced using LAVENT contains random error with $\sigma = 5$ s and systematic error with $a = 20$ s and $b = 0{\cdot}20$. Figure 9(a,b) shows that location errors and heat release rate error ratios found from an evaluation of the inverse algorithm based on LAVENT synthesized data are essentially indistinguishable from results of an evaluation of the inverse algorithm based on fire data interpolated from experimental measurements. In short, the use of computer simulated data will lead to realistic and useful estimates of the fire detection system's accuracy, as long as random and systematic errors of appropriate magnitude are included in the data.

The magnitudes of location and heat release rate ratio errors seen in Fig. 9(a,b) are instructive. Recall that the figures are based on the assumption of a fast-growing fire in a large ($20 \times 20 \times 3$ m) warehouse. Under these conditions, the inverse problem solution algorithm was able to locate 95% of the fires within 70 cm ($2/3d$) and 50% within 30 cm ($d/3$). Location accuracy for the inverse problem solution algorithm is quite good. The accuracy of the inverse algorithm in determining fire heat release rate is not as good. The inverse algorithm was able to determine the heat release rate of 95% of the fires to within a factor of five ($\varepsilon_Q = 0{\cdot}2$) and 50% of the fires within a factor of three ($\varepsilon_Q = 0{\cdot}33$). However, the heat release rate error ratios given in Fig. 9(b) are probably artificially low. The values of ε_Q (where $\varepsilon_Q = Q_{\mathrm{pred}}/Q_{\mathrm{act}}$) are too low because the values of actual heat release rate, Q_{act}, on which they are based are most likely too high. The values of actual heat release rate taken from Heskestad and Delichatsios[16] were determined by multiplying a measured rate of change of fuel mass by an estimated heat of combustion for the fuel. As a consequence a combustion efficiency of less than 100% in the test fire would result in an overestimate of Q_{act} and an underestimate of ε_Q.

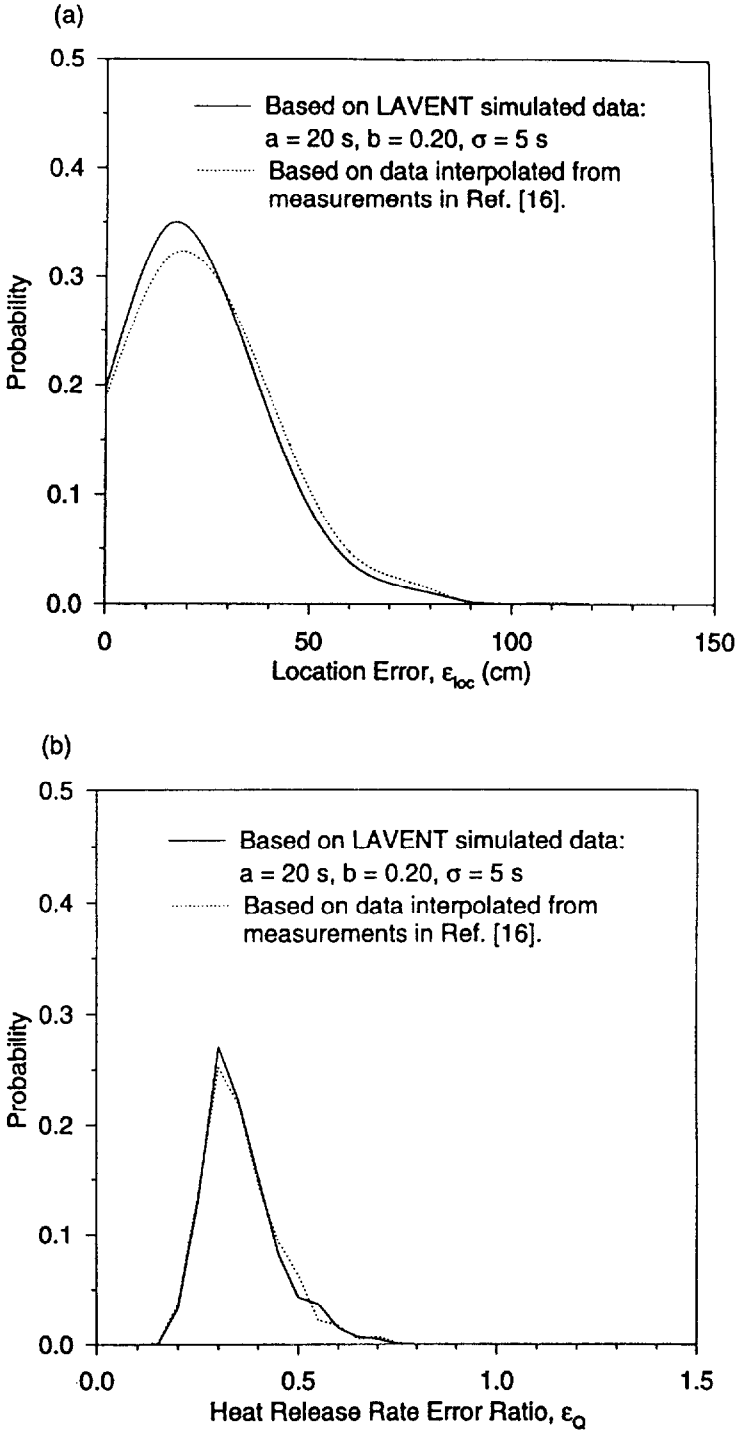

Fig. 9. (a) Comparison of location errors determined using LAVENT simulated data and data interpolated from measurements reported in Ref. 16. LAVENT data simulated with systematic error: $a = 20$ s, $b = 0{\cdot}2$, and random error: $\sigma = 5$ s. (b) Comparison of heat release rate errors determined using LAVENT simulated data and data interpolated from measurements reported in Ref. 16. LAVENT data simulated with systematic error: $a = 20$ s, $b = 0{\cdot}2$ and random error: $\sigma = 5$ s.

5 CONCLUSIONS

A proposed fire detection system based on the use of an inverse heat transfer problem solution algorithm capable of determining the location and heat release rate of an accidental compartment fire, has been described. The inverse problem solution algorithm uses as data the times of activation of temperature sensors distributed in an array on the ceiling of the compartment. The inverse problem solution algorithm then uses the fire model LAVENT as a forward model to predict the times of activation of the sensors for a given fire location and growth rate. The accidental fire is taken to be at the location and growth rate which minimizes the sum of squares of the residuals of measured and predicted sensor times of activation.

An evaluation of the inverse problem solution algorithm using computer simulated sensor activation times as data has demonstrated limits on the accuracy of the proposed fire detection system. The evaluation focused on the ability of the proposed fire detection system to locate and size accidental fires when systematic model errors in the forward problem solution and random measurement errors in the fire data were present. In particular, the evaluation showed that the accuracy of the inverse algorithm's location predictions was affected by the accuracy of the measurements of sensor activation times, but was not affected by the accuracy of the forward problem model. In contrast the accuracy of the inverse algorithm's heat release rate predictions was affected by both the accuracy of sensor activation time measurements and by the accuracy of the forward problem model. The effect of random errors in sensor activation time measurements was to widen the distribution of heat release rate error ratios. The effect of systematic errors in the forward problem solution was to shift the peak of the heat release rate error ratio distribution away from unity. The strong effect of model error on heat release rate predictions and the lack of any effect of model error on location predictions make the task of determining the heat release rate of a fire more challenging and more subject to error than the task of locating a fire.

An evaluation of the inverse problem solution algorithm using fire data interpolated from experimental measurements taken in a large-scale test burn, was compared to the evaluation relying on computer simulated fire data. Results of the two evaluations were shown to be similar to one another, when random and systematic errors of appropriate magnitude were applied to the simulated data. The comparison demonstrates the validity of the use of computer simulated data in the evaluation of the

inverse problem solution algorithm, as long as the simulated data incorporates realistic levels of error.

The evaluation of the inverse problem solution algorithm using interpolated fire data also indicated the level of accuracy that could be expected of the proposed fire detection system operating in a large scale industrial environment. The inverse problem solution algorithm was able to locate most fires within one-third of the distance between sensors and 95% of all fires within two-thirds of the distance between sensors. The algorithm was able to determine the heat release rate of most fires to within a factor of three and the heat release rate of 95% of all fires to within a factor of five.

ACKNOWLEDGEMENT

This work has been supported by the Building and Fire Research Laboratory of NIST through contract number 60NANB2D1290, Dr W.L. Grosshandler, scientific officer.

REFERENCES

1. Okayama & Yoshiaki, *Fire Safety Journal*, **17**(6) (1991) 535–553.
2. Meacham, B. J., *Journal of Fire Protection Engineering*, **6**(3) (1994) 125–136.
3. Milke, J. A. & McAvoy, T. J., *Fire Technology*, **31**(2) (1995) 120–136.
4. Mueller, H. C. & Fischer, A., *Proceedings of the 29th Annual International Carnahan Conference on Security Technology, IEEE*, Sanderstead, UK, October 1995, pp. 197–204.
5. Heskestad, G. & Newman, J. S., *Fire Safety Journal*, **18**(4) (1992) 355–374.
6. Milke, J. A., McAvoy, T. J. & Kunt, T., *Proceedings International Conference on Fire Research and Engineering*, Orlando, FL, September 1995, pp. 301–306.
7. Jandeweith, T., *Proceedings of the 29th Annual International Carnahan Conference on Security Technology, IEEE*, Sanderstead, UK, October 1995, pp. 205–208.
8. Jarny, Y., Ozisik, M. N. & Bardon, J. P., *International Journal of Heat and Mass Transfer*, **34** (1991) 2911–2919.
9. Padakannaya, K., Richards, R. F.& Plumb, O. A., *Proceedings of the 30th National Heat Transfer Conference*, ed. W. J. Bryan & J. V. Beck, HTD-Vol. 312, 1995, pp. 63–70.
10. Moutsoglu, A., *Journal of Heat Transfer*, **111** (1989) 37–43.
11. Falco, L. & Debergh, P., AUBE '89, University of Duisburg, Germany, October 1989.
12. Brenci, M., Guzzi, D., Mencaglia, A. & Grazia, A., *Measurement*, **12**(2) (1993) 183–190.

13. Richards, R. F., Ribail, R. T., Bakkom, A. W. & Plumb, O. A., *Fire Safety Journal*, **28**(4) (1997) 351–378 (this issue).
14. Heskestad, G., Society of Fire Protection Engineers, Technology report 82-8, 1982.
15. Cooper, L. Y., *Fire Safety Journal*, **16** (1990) 137–163.
16. Heskestad, G. & Delichatsios, M. A., 17*th Symposium* (*International*) *on Combustion*, 1985, pp. 1113–23.